Volume 1 | Number 1 | Jan 2013 | Pages 1–100

Journal of
Materials Chemistry A

Materials for energy and sustainability
www.rsc.org/materialsA

Li⁺

ROYAL SOCIETY
OF CHEMISTRY

ROYAL SOCIETY
OF CHEMISTRY

www.rsc.org/materialsA

Journal Name

ARTICLE

Photo-directed growth of Au nanowires on ZnO arrays for enhancing photoelectrochemical performances

Teng Wang,[a] Bingjun Jin,[a] Zhengbo Jiao,[a] Gongxuan Lu,[a] Jinhua Ye,[b] and Yingpu Bi[*a]

Herein, we demonstrate that ZnO nanowire arrays could be rationally connected with each other by thin Au nanowires to construct a novel cross-linked hetero-structure by a simple photo-directed growth strategy. Moreover, a possible formation mechanism of this Au/ZnO hierarchical nanostructure has been proposed. In the case of light irradiation, the rapid electron enrichment on the top (002) facets of ZnO nanowires will result in the high concentration holes on side facets, which could generate a positive electric field. As a result of the electronegativity, $[Au(OH)_xCl_{4-x}]^-$ (where x = 0-4) anions could be pulled in this electric field and reduced on side facets of ZnO nanowires, and the Au nanowires could be gradually formed through an exact opposite point growth route. Furthermore, the photoelectrochemical performance studies clearly reveal that these novel cross-linked hetero-arrays exhibit much higher visible light photocurrent density than both pure ZnO nanowire arrays and traditional Au nanoparticles/ZnO nanowire heterostructures, which may be primarily ascribed to the efficient electron transfer from Au nanostructures into ZnO nanowires.

1. Introduction

Recently, ZnO nanowire arrays have shown great potentials for solving the worldwide environmental pollution and energy crisis due to their excellent properties such as high surface-to-volume ratio, efficient charge transport, nontoxicity etc.[1, 2] As results of these merits, ZnO nanowire arrays can be applied as ultraviolet (UV) lasers,[3, 4] high performance nanosensors,[5] photocatalysts,[6] solar cells,[7, 8] piezoelectric nanogenerators etc.[9] However, owning to their large band gap (3.4 eV), the intrinsically poor visible light utilization and high recombination rate of photogenerated electron-hole pairs greatly restrict their future practical applications in photocatalysis and photoelectron conversion. To address these issues, much effort has been recently devoted to the exploration of effective strategies, including hydrogenation,[10] doping,[11] and coating with other materials,[12-17] etc.

More recently, the noble metal nanoparticle decorated ZnO nanowire arrays have aroused great interest due to the fact that noble metal can effectively promote the charge separation and excite surface plasmon resonance at the visible region.[18-21] Among these noble metals, Au nanoparticles tend to be a better choice owing to their properties of being relatively stable, catalytically active and optically sensitive. For example, Wu

and co-workers reported better photo-degradation ability of Au nanoparticles grafted ZnO nanowire arrays via photo-reduction method compared to the pure ZnO nanowire arrays.[22, 23] Moreover, Zhao et al. presented that the optimal Au/ZnO hybrids, synthesized through hydrothermal method, displayed complete photocatalytic degradation of methyl blue within 60 min.[24] However, the as-reported nanocomposites either suffered from the aggregation of Au nanoparticles, which hindered the realization of high photocatalytic efficiency, or synthesized through a complex method. Moreover, Au nanoparticles cannot transfer the excessive photogenerated charge carriers from original ZnO nanowire to the near ones, which may have less charge carriers (induced by the difference of light irradiation and morphology) and thus lower recombination rate. The unbalanced system will result in a poor photocatalytic activity. Thereby, it is still a great challenge to design and construct novel heterostructured Au/ZnO nanowire arrays for effectively separating the photoexcited electron-hole pairs and enhancing the visible light utilization.

Herein, we report a feasible approach to resolve the above issues by connecting the ZnO nanowires with each other via thin Au nanowires to form a cross-linked heterostructure by simple photo-directed growth process. Furthermore, the structure, position, amount, and size of Au nanoproducts can be

further rationally tailored by adjusting the reaction parameters. In addition, the photoelectrochemical studies reveal that the photocurrent of cross-linked Au/ZnO nanowire arrays were strengthened dramatically, compared with both pure ZnO nanowire arrays and traditional Au nanoparticles/ZnO nanowire heterostructures, which may be due to the rapid electron transfers among ZnO nanowires via thin Au nanowires and reducing the recombination probability of photoexcited electron-hole pairs.

2. Experimental

2.1 Materials

All the chemicals were of analytical grade and used as received without any further purification, unless otherwise stated. All chemicals were purchased from Sinopharm Group Chemical Reagent Co. Ltd. China. Deionized water with a resistivity of 18.25 MΩ.cm was used in all reactions. Indium-tin oxide (ITO)-coated glasses were purchased from Zhuhai Kaivo Electronic Components Co., Ltd. China.
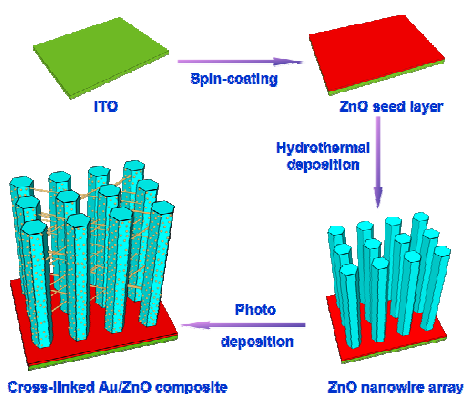
Scheme 1 Schematic illustration of the fabrication of Au/ZnO heterostructure nanowire arrays.

2.2 Preparation of the cross-linked Au/ZnO nanowire arrays

Preparation of the ZnO nanowire arrays. The ZnO nanowire arrays were synthesized via the method employed in our previous report.[19] In the first step, 1.2 M zinc acetate dehydrate [$Zn(CH_3COO)_2 \cdot 2H_2O$] sol dissolved in ethylene glycol monomethyl ether [$CH_3O-CH_2-CH_2OH$] with equal amount of diethanolamine (DEA) added. After that, the sol was spin-coated on an ITO-coated glass substrate using a vacuum spin coater (VTC-100) followed by a drying procedure. After the repeated spin-coating process, the as-prepared thin film was calcined in a muffle furnace in the air at 350 °C for 30 min to obtain the ZnO seed layer. Then the coated substrate with the coating side upside-down was immersed in the aqueous solution containing 0.04 M zinc nitrate ($Zn(NO_3)_2 \cdot 6H_2O$) and 0.04 M hexamethylene tetraamine (HMT) contained in a Telflon liner stainless-steel autoclave to grow ZnO nanowire arrays at 95 °C for 6 h. The achieved final product was then intensively rinsed with deionized water and absolute ethyl alcohol for several times followed by a drying step in an oven at 60 °C.

Preparation of cross-linked Au/ZnO heteronanostructure. The Au modified ZnO nanowire arrays were prepared by a simple photo-reduction method. The as-prepared ZnO nanowire arrays were immersed in chloroauric acid ($HAuCl_4$, 0.4 mM) aqueous solution containing 0.1 M Na_3PO_4 and 0.3 M Polyvinylpyrrolidone (PVP), and then illuminated by a 300 W Xe lamp (HSX-F/UV 300) for 2 minutes to reduce the Au(III) near the zinc oxide nanowires to Au nanoparticles. Then the as-prepared heterostructures were rinsed with deionized water and absolute ethyl alcohol for several times to remove the residual and dried at 60 °C in the air.

2.3 Characterization.

The morphology and elemental distributions of the products were characterized by field emission scanning electron microscope (FESEM, JSM-6701F, JEOL) employing an accelerating voltage of 5.00 kV with an energy dispersive spectrometer (EDS). X-ray diffraction analysis (XRD, Rigaku RINT-2000) using Cu Kα radiation at 40 k eV and 40 mA was employed to identify the crystalline structure of our as-prepared products. X-ray photoelectron spectroscopy (XPS) was performed by a ESCALAB250xi photoelectron spectrometer with X-Ray Monochromatisation as the excitation source to analyze samples' elemental composition. The UV-Vis absorption spectra were carried out with a spectrophotometer (UV-2550, SHIMADZU, Japan). And the Photoluminescence (PL) spectra were measured at room temperature using an F-7000 spectrofluorometer (Hitachi High-Technologies, Tokyo, Japan) with the excitation wavelength (EX) fixed at 325 nm.

2.4 Characterization of Water-Splitting Photoelectrode

The photoelectrochemical properties of bare ZnO nanowire arrays and the Au/ZnO heterojunctions were measured through a typical 3-electrode system, in which a piece of Pt foil (3× 2cm) and a saturated calomel electrode (SCE) were used as counter and reference electrodes, respectively. And the as-prepared ZnO nanowire array and Au/ZnO nanowire array photoanodes were employed to be the working electrodes with a surface area of 2 cm^2, respectively. The whole photoelectrochemical tests were operated in 40 mL electrolyte medium containing 0.1 M Na_2SO_4 and 5 mL methanol, and the data was gathered by an electrochemical workstation (CHI660D). A 300 W Xe lamp (HSX-F/UV 300) with an ultraviolet-cut filter was used as the resource of visible light illumination. Linear sweep voltammograms were measured under a bias voltage between -0.2 V and +1.0 V (vs.SCE) with a scan rate of 0.1 V/s. Amperometric i-t curves were tested at a bias voltage of +0.2 V (vs. SCE), respectively.

3. Results and Discussion

The ZnO nanowire arrays have been firstly synthesized via a reported hydrothermal method[19]. As shown in Figure 1A, the

typical scanning electron microscopy (SEM) images clearly indicate that the obtained ZnO nanowires are vertically aligned into well-defined arrays with a high surface density (ca. 10^9 wires cm^{-2}). Moreover, it can be observed that the as-synthesized ZnO nanowires have lengths of ca. 2 μm and diameters range from 100 to 150 nm. Interestingly, when the ZnO nanowire arrays were immersed into the HAuCl$_4$ aqueous solution and irradiated under the light, the dissociated Au(III) ions were gradually reduced to Au nanoparticles and formed on the surface of zinc oxide nanowires. Further increasing the reaction time, the opposite Au nanoparticles have been transformed into nanorods and finally connected with each
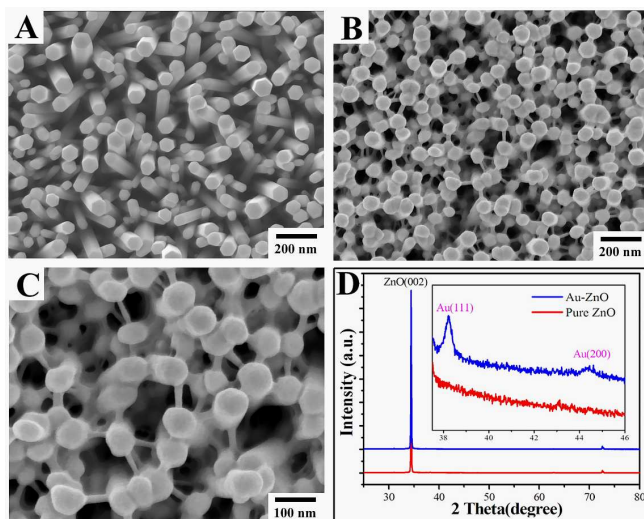

Figure 1 (A) SEM images of pure ZnO nanowire arrays; (B, C) cross-linked Au/ZnO nanowire arrays under different magnifications, respectively; (D) XRD pattern of ZnO nanowire arrays and cross-linked Au/ZnO nanowire arrays, the inset close-up plot of the Au XRD peak region.

other to form thin nanowires. As shown in Figure 1B, 1C, and S1, the separated ZnO nanowires are connected with each other by numerous thin Au nanowires to construct a novel cross-linked heterostructure (shown in Figure S2). Furthermore, the compositions and crystalline structure of cross-linked Au/ZnO hetero-arrays and pure ZnO nanowire arrays have been studied by X-ray diffraction (XRD). It can be clearly observed from Figure 1D that after photo-induced growth, the main ZnO diffraction peaks in the hetero-arrays have no evident changes compared with pure hexagonal ZnO nanowire arrays. Furthermore, the intense peak at 2θ = 34.52° is assigned to the (002) plane of the ZnO nanowires, demonstrating that the ZnO nanowires are vertically aligned with each other. The inset in Figure 1D provides additional XRD detail on the 38° to 46° 2θ scan range and reveals smaller peaks at 38° and 44° which correspond to the (111) and (200) plane of gold nanostructure precipitated on the surfaces of ZnO nanowires, respectively. Thus, these demonstrations clearly confirm that Au nanostructures have been successfully deposited on the ZnO nanowires to form a cross-linked heterostructure.

To obtain a further insight into the formation of Au/ZnO nanowire hetero-nanoarrays, X-ray photoelectron spectroscopy

(XPS) was applied to analyse its surface composition, in which C1s (284.8 eV) was used to calibrate the binding energies. As shown in Figure 2A, the full XPS spectrum reveals the existence of Zn, O, Au, and C elements, further elucidating that the cross-linked Au/ZnO nanowire arrays are successfully obtained without any impurity existed. The high resolution XPS spectrum of Zn 2p shown in Figure 2B clearly indicates that the two peaks positioned at 1021.8 eV and 1044.8 eV are correspond to Zn 2p$_{3/2}$ and Zn 2p$_{1/2}$, respectively. And the energy difference between these two peaks is 23.0 eV, clearly illustrating that zinc species is in the formal Zn^{2+} valence state. Moreover, the binding energies of O 1s are presented in Figure 2C, which can be fitted to two peaks obtained from the curve fitting of the data. The peak located at about 530.6 eV is associated with lattice oxygen of ZnO, whereas the weaker shoulder peak at about 531.9 eV can be attributed to chemisorbed oxygen caused by the surface hydroxyl groups. Furthermore, the high resolution XPS spectrum in Figure 2D has been fitted to four peaks. The two peaks centred at 83.6 eV and 87.3 eV are attributed to Au 4f$_{7/2}$ and 4f$_{5/2}$, which exhibit a negative shift of 0.2 eV in comparison to 83.8 eV of bulk Au. It is generally believed that this slight shift is caused by electron transfer from plasmonic Au thin nanowires to ZnO nanowire arrays due to the strong electronic interaction between Au and oxide support, which has also been reported by other research groups.[24-27] Moreover, it should be noted that the other peaks centred at 88.9 eV and 91.9 eV are corresponded to Zn 3p$_{3/2}$ and Zn 3p$_{1/2}$. On the basis of above results, it can be concluded that XPS analysis clearly confirms the realization of the special network Au/ZnO hetero-nanoarrays, which is in good agreement with the SEM and XRD results. In addition, the energy-dispersive X-ray spectroscopy (EDS) of cross-linked Au/ZnO nanowire arrays has also been studied and shown in Figure S3, confirming that except for the Au Zn, and O elements, no other impurity has been detected.
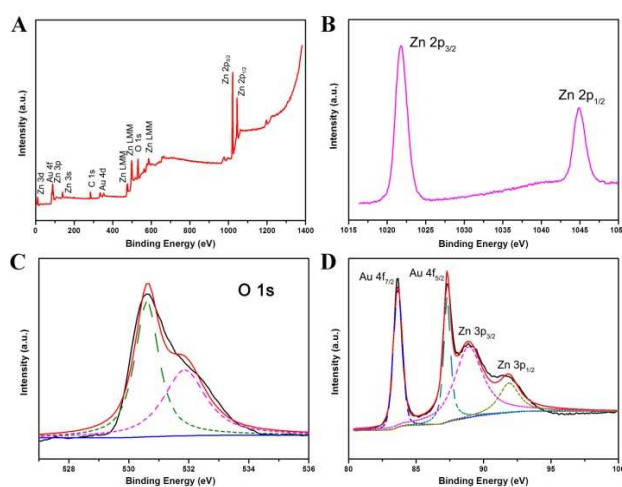

Figure 2 (A) Wide XPS spectrum and high resolution XPS spectra of (B) Zn 2p, (C) O1s and (D) Au 4f of cross-linked Au/ZnO nanowire arrays.

Furthermore, note that both Na$_3$PO$_4$ and PVP play crucial roles on the formation of cross-linked Au/ZnO heterostructure.

Herein, some comparison experiments have been designed to elucidate the morphology variety of as-prepared Au/ZnO heterostructures. As shown in Figure 3A, the addition of both reagents results in a perfectly network nanostructure. However, in the absence of Na_3PO_4, only irregular Au nanoparticle aggregates have been grafted on the surfaces of ZnO nanowires and no any thin gold nanowire has been formed (Figure 3B). Furthermore, when PVP was taken out from this reaction system, only separated Au nanoparticles
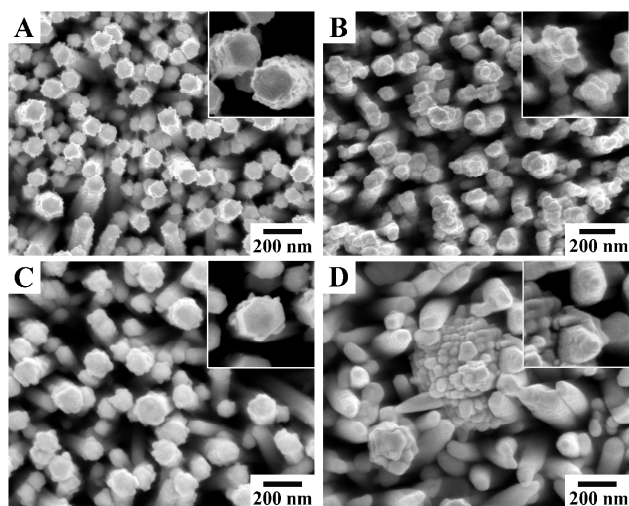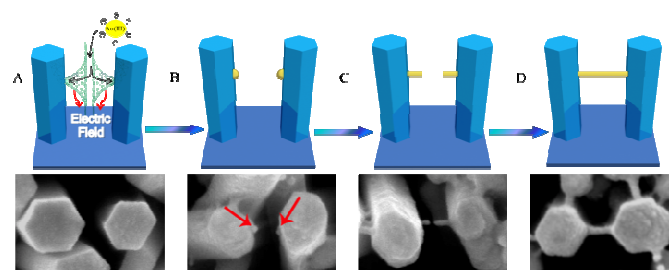

Figure 3 SEM images of Au/ZnO nanowire arrays reacted in 0.4mM $HAuCl_4$, 0.1 M Na_3PO_4 and 0.3 M PVP (A), 0.4mM $HAuCl_4$ and 0.3 M PVP (B), 0.4mM $HAuCl_4$ and 0.1 M Na_3PO_4 (C), and only 0.4mM $HAuCl_4$ aqueous solution(D), respectively. The insets show the magnified images.

were deposited on the side surface of ZnO nanowire (Figure 3C). In contrast, in the absence of both Na_3PO_4 and PVP, as indicated in Figure 3D, only aggregated and large Au nanoparticles have been produced, and the zinc oxide nanowires have also been eroded into cone-like nanorods. It has been reported that Zn^{2+} ions on the outmost layer of ZnO nanowire can strongly interact with PO_4^{3-} which can hinder the deposition of Au nanostructures. Thereby, the deposition sites for Au nanoparticles on ZnO nanowires have been greatly reduced, especially for the top (002) facets whose outmost layer consists of Zn^{2+}. Furthermore, according to the report of Kung et al,[28] the chloroauric anion would hydrolyze to form $[Au(OH)_xCl_{4-x}]^-$ (where x = 0-4) in alkaline solution, which is favourable for the formation of small Au nanoparticles. Thereby, in the presence of Na_3PO_4, which provides an alkaline environment, Au could be reduced to small sized nanoparticles and deposited separately on the surface of ZnO nanowires under irradiation. In addition, we have also studied the effect of PVP concentrations on the formation of Au/ZnO nanostructure, and the results have been shown in Figure S4 and Figure S5, respectively. It can be clearly seen that decreasing PVP concentration is disadvantageous for the formation of Au thin nanowires on ZnO nanowires. Based on the above results, it can be concluded that sodium orthophosphate, PVP as well as its concentration control are both essential for the formation of cross-linked Au/ZnO nanowire arrays.

To further illustrate the effect of pH value on the formation process of the thin Au nanowires, Na_3PO_4 has been replaced by Na_2HPO_4 and NaH_2PO_4, respectively, during the photo-reduction process. As shown in Figure S6A, the networked hetero-structure with less Au nanowires could also be formed in the presence of Na_2HPO_4, and few Au nanoparticles have been grafted on the surfaces of ZnO nanowires. However, when NaH_2PO_4 was introduced, only irregular nanowires with rough surfaces have been obtained and no any Au nanowires have been observed on the nanoproducts (Figure S6C). As shown in the XRD results, it has been found that $Zn_3(PO_4)_2$ nanoshells have been formed on the ZnO nanowire arrays instead of thin Au nanowires. The above results clearly reveal that appropriately alkaline pH value could facilitate the formation of thin Au nanowires on the ZnO nanowire arrays.

Scheme 2 Schematic illustration and SEM images of the formation process of cross-linked Au/ZnO nanowire arrays

Based on the observed experimental results, we proposed a potential reaction route explaining the formation of the cross-linked network nanostructures.[29] The schematic illustration for the growth process is presented in Scheme 2. It has been reported that in the case of irradiation, the photogenerated electrons would accumulate on the top facets of the ZnO nanowire,[19] which means that the photoexcited holes are mainly distributed on the side of ZnO nanowires. This separation and accumulation process of photo-excited charges at different locations would therefore form a surface electric field. Thereby, a positive electric field, caused by the photoexcited holes, would be formed on the side surface of ZnO nanowires. When two nanowires get close enough, the electric fields of the nanowires will interact with each other to form a strong electric field force, just like the illustration shown in Scheme 2A (see the enlarged graph in Figure S8). This symmetrical electric field tends to attract negative charges to the photogenerated hole centres located on both sides along the direction depicted in Scheme 2A. Thereby, the negatively charged $[Au(OH)_xCl_{4-x}]^-$ would be simultaneously attracted to the surface of both nanowires under the direction of the electric field. Simultaneously, with the assistance of Na_3PO_4 and PVP, which can slow down the deposition process, avoid nanoparticles' aggregation and maintain an anisotropic growth trend, the Au nanowires will be gradually produced. However, the more detailed formation mechanism of this cross-linked heterostructure cannot be completely understand and still needs further investigations.

Moreover, the UV-vis light absorption spectrums of Au nanowires connected ZnO nanowire arrays (shown in Figure S9) has been explored. For comparison, the optical properties of pure ZnO nanowire arrays (shown in Figure 1A) and general Au nanoparticle modified ZnO nanowire arrays (shown in Figure 3C) have also been performed. As shown in Figure 4, it can be clearly seen that the pure ZnO nanowire arrays show a steep absorption at wavelength shorter than 400 nm, revealing that the as-prepared ZnO nanowire arrays are transparent in the visible region. On the contrary, the transmittance in the visible
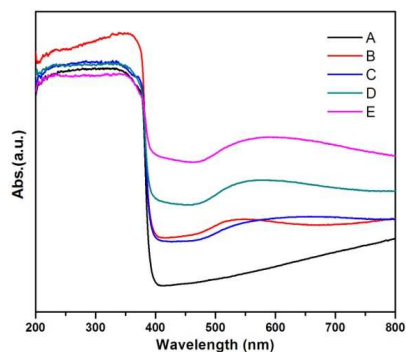

Figure 4 UV–visible light absorption spectra of the ZnO nanowire arrays (A), Au/ZnO nanowire arrays with only Au nanoparticles (B) and cross-linked Au/ZnO nanowire arrays with different Au deposition (0.4 mM (C), 0.8 mM (D), 1.2 mM (E) HAuCl₄ was used in the reaction, respectively).

wavelength (400-750 nm) decreased drastically after the modification of Au nanostructures, especially at the wavelength larger than 500 nm. The enhanced absorption of visible light should be caused by the surface plasmon resonance (SPR) of Au nanostructures. Furthermore, in comparison with the general Au nanoparticle deposited ZnO nanowire arrays, the absorption of cross-linked Au/ZnO nanohybrids is greatly broadened and red-shifted with tens of nanometers due to the SPR of special Au nanostructures with complex shapes and various sizes.[30] Thus, it can be concluded that this new nanostructure will make the usage of solar power more efficient. Moreover, it also indicates that the absorption of visible light can be further enhanced as the content of Au increasing.
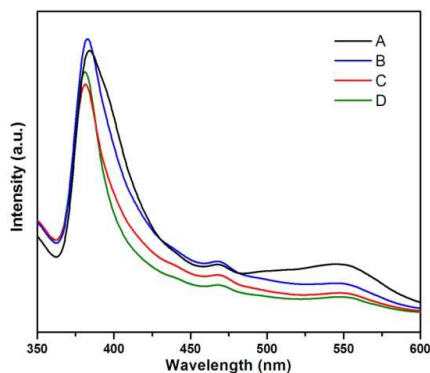

Figure 5 Room temperature PL spectra of ZnO nanowire arrays (A) and cross-linked Au/ZnO nanowire arrays with different Au deposition (0.4 mM (B), 0.8 mM (C), 1.2 mM (D) HAuCl₄ was used in the reaction, respectively).

To further observe optical performances of the Au/ZnO heterostructures, the room temperature photoluminescence (PL) spectra of pure ZnO nanowire arrays and Au/ZnO nanohybrids are achieved and presented in Figure 5. The spectra exhibit two main emission bands centred at around 380 nm and 550 nm, respectively. Among them, the UV emission band centred at 380 nm should be caused by the excitonic recombination within ZnO. According to the previous reports,[23, 31, 32] the visible emission band centred at 550 nm is attributed to an electronic transition from the defect-associated trap states, such as oxygen vacancies, to deeply trapped holes near or in the valence band of ZnO. In addition, it can be clearly seen that the PL intensity of cross-linked Au/ZnO nanowire arrays is relatively weak and gets weaker as the amount of Au increasing compared to pure ZnO. The quenching of the visible emission should be ascribed to the strong absorption of Au nanostructures in the visible light range due to the SPR of Au. Moreover, Au nanostructures can deposit in oxygen vacancies or defects on the surface of ZnO nanowire and prevent the electronic transition, leading to a further decrease of the visible emission. On the other hand, it is generally believed that the transfer of electrons from the conduction band of zinc oxide to the gold nanostructures should be the reason for the quenching of the UV emission. In the field of photocatalysis research, the decreasing of PL intensity generally indicates better photocatalyitc properties. Based on these results mentioned in the UV-vis light absorption spectra and the PL spectra, we speculate that the cross-linked Au/ZnO nanowire arrays possibly own a better photocatalytic and photoelectrochemical property than the pure ZnO nanowire arrays.
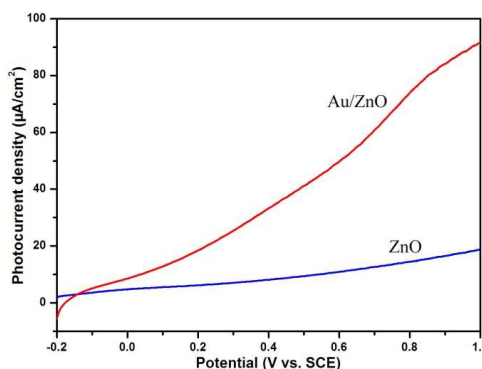

Figure 6 Linear sweep voltammograms of the ZnO nanowire arrays and cross-linked Au/ZnO heterostructures under visible light illumination with the voltage ranged from -0.2 V to +1.0 V (vs. SCE).
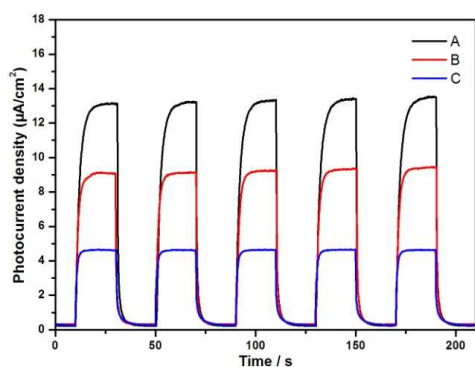
Figure 7 Amperometric I–t curves of the ZnO nanowire arrays (C), Au nanoparticle tuned ZnO nanowire arrays (B), and cross-linked Au/ZnO nanowire arrays reacted in 0.4 mM HAuCl$_4$, 0.1 M Na$_3$PO$_4$ and 0.3 M PVP (A) at an applied voltage of +0.2V with 20 s light on/off cycles under visible light irradiation.

The photoelectric performances of as-prepared Au/ZnO nanowire nanohybrids have been investigated under visible light irradiation, which has been rarely studied but very meaningful for the full utilization of solar energy. For comparison, the photoelectrochemical properties of pure and Au nanoparticle tailored ZnO nanowire arrays (see Figure 3C) have also been explored. As shown in Figure 6, it can be clearly seen that the cross-linked Au/ZnO nanowire array shows a much higher photocurrent density compared to pure ZnO nanowire array. In addition, Figure 7 further demonstrates that the photocurrent density of the ZnO nanowire array enhanced remarkably after modification with Au nanostructures. The maximum photocurrent density of cross-linked Au/ZnO hybrids amounts to 13.0 μA/ cm^2, much higher than both pure ZnO nanowire arrays and the general Au nanoparticle tuned ZnO nanowire arrays, revealing a much better performance. Furthermore, as shown in Figure S10, increasing the amount of Au can further enhance the photocurrent density of the cross-linked Au/ZnO heterostructure, confirming the positive effects of Au nanostructures. However, further increasing the amount of Au nanostructures, the light response slows down, indicating an unstable photoelectric state. This may be ascribed to the transient accumulation of mass photoexcited charges. For this reason, the percentage of Au nanostructures should be controlled in an available range in order to gain a high photocurrent density and stability at the same time. Furthermore, the stability properties of the cross-linked Au/ZnO heterostructure under chopped and continuous light illumination have also been explored (shown in Figure S11 and Figure S12), indicating a pretty good stability. The above results clearly reveal that the cross-linked Au/ZnO nanowire arrays exhibit much better photoelectric activities compared to both pure and general Au nanoparticles grafted ZnO nanowire arrays. Therefore, this method could serve as a facile and effective strategy for the enhancement of visible light photocurrent.
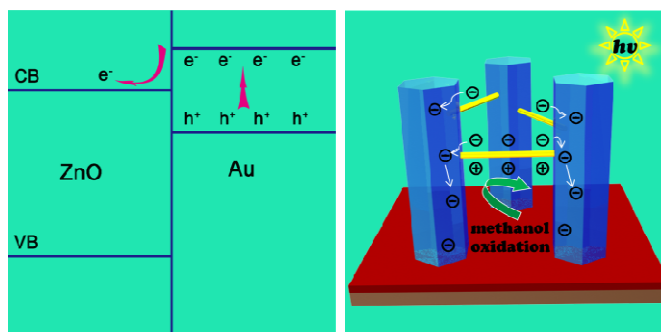
Scheme 3 Schematic illustration of the enhanced visible light photocurrent density for the as-prepared cross-linked Au/ZnO heterostructures.

The enhancement of photoelectric activity of the cross-linked Au/ZnO nanowire arrays should be ascribed to the Plasmon-induced charge separation and transmission.[30, 33-36] And the schematic illustration of the proposed mechanism is illustrated in scheme 3. Metal nanoparticles are usually applied to sink photogenerated electrons from semiconductors. However, in the case of visible light, the gold nanostructures can generate hot electrons induced by the SPR and inject them into the conduction band of adjacent ZnO nanowires, enhancing the photoelectric performance. Unlike the Au nanoparticles, Au nanowires can transport the hot electrons more efficiently and absorb more visible light due to their large surface areas and the enlarged visible light absorption range, which further improve the photoelectric properties. Moreover, the oxidized gold nanowires could be reduced immediately by the nearby sacrificial reagent (Here, the methanol was used) in the solution, ensuring the constant generation of hot electrons. However, due to the fact that SPR-induced electron transformation on metals is affected by many factors in the plasmonic-photocatalyst system, deeper investigation for the enhancement mechanism is required in the future. Nevertheless, we can make sure that the visible light photoelectrochemical properties of the ZnO nanowire arrays could be greatly enhanced through Au modification.

4. Conclusion

In summary, we have demonstrated a facile and efficient strategy for the fabrication of cross-linked Au/ZnO nanowire array heterostructures. Moreover, the heterostructures' growth mechanism has been investigated and proposed by changing reaction parameters. Besides, the cross-linked Au/ZnO nanowire arrays could also be further tuned by changing pH value more accurately. In addition, the adsorbed Au nanostructures could inject hot electrons into the conduction band of ZnO nanowire based on the surface plasmon resonance under visible light irradiation, enhancing the photoelectric performance. This specific cross-linked nanostructure might also be promising in various potential applications including photo-energy conversion and even surface enhanced Raman scattering. More importantly, we believe that this facile

synthetic method can also be used for the formation of other metal/semiconductor heterostructures.

Acknowledgements

Notes and references

a. State Key Laboratory for Oxo Synthesis & Selective Oxidation, and National Engineering Research Center for Fine Petrochemical Intermediates, Lanzhou Institute of Chemical Physics, CAS, Lanzhou 730000, China. E-mail: yingpubi@licp.cas.cn

b. International Center for Materials Nanoarchitectonics (MANA), and Research Unit for Environmental Remediation Materials, National Institute for Materials Science, Tsukuba, 305-0047, Japan.

† Electronic Supplementary Information (ESI) available: Experimental section, additional figures and discussions. See DOI: 10.1039/b000000x/

1   S. Xu and Z. L. Wang, *Nano Res.*, 2011, **4**, 1013-1098.

2   B. Weintraub, Z. Zhou, Y. Li and Y. Deng, *Nanoscale*, 2010, **2**, 1573-1587.

3   L. E. Greene, M. Law, J. Goldberger, F. Kim, J. C. Johnson, Y. Zhang, R. J. Saykally and P. Yang, *Angew. Chem.*, 2003, **42**, 3031-3034.

4   P. Yang, H. Yan, S. Mao, R. Russo, J. Johnson, R. Saykally, N. Morris, J. Pham, R. He and H.-J. Choi, *Adv. Funct. Mater.*, 2002, **12**, 323-331.

5   X. Wang, X. Wang, C. J. Summers and Z. L. Wang, *Nano Lett.*, 2004, **4**, 423-426.

6   J. L. Yang, S. J. An, W. I. Park, G. C. Yi and W. Choi, *Adv. Mater.*, 2004, **16**, 1661-1664.

7   C. Xu, J. Wu, U. V. Desai and D. Gao, *J. Am. Chem. Soc.*, 2011, **133**, 8122-8125.

8   M. Law, L. E. Greene, J. C. Johnson, R. Saykally and P. Yang, *Nat. Mater.*, 2005, **4**, 455-459.

9   W. Han, Y. Zhou, Y. Zhang, C.-Y. Chen, L. Lin, X. Wang, S. Wang and Z. L. Wang, *ACS nano*, 2012, **6**, 3760-3766.

10 X. Lu, G. Wang, S. Xie, J. Shi, W. Li, Y. Tong and Y. Li, *Chem. Commun.*, 2012, **48**, 7717-7719.

11 G. D. Yuan, W. J. Zhang, J. S. Jie, X. Fan, J. X. Tang, I. Shafiq, Z. Z. Ye, C. S. Lee and S. T. Lee, *Adv. Mater.*, 2008, **20**, 168-173.

12 H. M. Chen, C. K. Chen, C. C. Lin, R.-S. Liu, H. Yang, W.-S. Chang, K.-H. Chen, T.-S. Chan, J.-F. Lee and D. P. Tsai, *J. Phys. Chem. C*, 2011, **115**, 21971-21980.

13 C.-H. Hsu and D.-H. Chen, *Int. J. Hydrogen Energy*, 2011, **36**, 15538-15547.

14 Y. Myung, D. M. Jang, T. K. Sung, Y. J. Sohn, G. B. Jung, Y. J. Cho, H. S. Kim and J. Park, *ACS Nano*, 2010, **4**, 3789-3800.

15 H. M. Chen, C. K. Chen, Y. C. Chang, C. W. Tsai, R. S. Liu, S. F. Hu, W. S. Chang and K. H. Chen, *Angew. Chem. Int. Ed.*, 2010, **49**, 5966-5969.

16 Z.-Q. Liu, X.-H. Xie, Q.-Z. Xu, S.-H. Guo, N. Li, Y.-B. Chen and Y.-Z. Su, *Electrochim. Acta*, 2013, **98**, 268-273.

17 Y.-Z. Su, K. Xiao, Z.-J. Liao, Y.-H. Zhong, N. Li, Y.-B. Chen and Z.-Q. Liu, *Int. J. Hydrogen Energy*, 2013, **38**, 15019-15026.

18 Y. Wei, J. Kong, L. Yang, L. Ke, H. R. Tan, H. Liu, Y. Huang, X. W. Sun, X. Lu and H. Du, *J. Mater. Chem. A*, 2013, **1**, 5045-5052.

19 T. Wang, Z. Jiao, T. Chen, Y. Li, W. Ren, S. Lin, G. Lu, J. Ye and Y. Bi, *Nanoscale*, 2013, **5**, 7552-7557.

20 Y. M. Chang, M. L. Lin, T. Y. Lai, H. Y. Lee, C. M. Lin, Y. C. Wu and J. Y. Juang, *ACS Appl. Mat. Interfaces*, 2012, **4**, 6676-6682.

21 Z. H. Chen, Y. B. Tang, C. P. Liu, Y. H. Leung, G. D. Yuan, L. M. Chen, Y. Q. Wang, I. Bello, J. A. Zapien, W. J. Zhang, C. S. Lee and S. T. Lee, *J. Phys. Chem. C*, 2009, **113**, 13433-13437.

22 J.-J. Wu and C.-H. Tseng, *Appl. Catal., B*, 2006, **66**, 51-57.

23 L. Sun, D. Zhao, Z. Song, C. Shan, Z. Zhang, B. Li and D. Shen, *J. Colloid Interface Sci.*, 2011, **363**, 175-181.

24 T. H. Yang, L. D. Huang, Y. W. Harn, C. C. Lin, J. K. Chang, C. I. Wu and J. M. Wu, *Small*, 2013, **9**, 3169-3182.

25 M. Ahmad, S. Yingying, A. Nisar, H. Sun, W. Shen, M. Wei and J. Zhu, *J. Mater. Chem.*, 2011, **21**, 7723-7729.

26 X.-j. Wang, W. Wang and Y.-L. Liu, *Sens. Actuators, B*, 2012, **168**, 39-45.

27 J. Zhang, X. Liu, S. Wu, B. Cao and S. Zheng, *Sens. Actuators, B*, 2012, **169**, 61-66.

28 H. Kung, *J. Catal.*, 2003, **216**, 425-432.

29 F. Vietmeyer, M. P. McDonald and M. Kuno, *J. Phys. Chem. C*, 2012, **116**, 12379-12396.

30 S. Linic, P. Christopher and D. B. Ingram, *Nat. Mater.*, 2011, **10**, 911-921.

31 C. W. Cheng, E. J. Sie, B. Liu, C. H. A. Huan, T. C. Sum, H. D. Sun and H. J. Fan, *Appl. Phys. Lett.*, 2010, **96**, 0711071-0711073.

32 X. Hou, L. Wang, G. He and J. Hao, *CrystEngComm*, 2012, **14**, 5158-5162.

33 W. B. Hou and S. B. Cronin, *Adv. Funct. Mater.*, 2013, **23**, 1612-1619.

34 Y. Tian and T. Tatsuma, *Chem. Commun.*, 2004, 1810-1811.

35 Y. Tian and T. Tatsuma, *J. Am. Chem. Soc.*, 2005, **127**, 7632-7637.

36 Z. Zhang, L. Zhang, M. N. Hedhili, H. Zhang and P. Wang, *Nano Lett.*, 2013, **13**, 14-20.

Photo-directed growth of Au nanowires on ZnO arrays for

enhancing photoelectrochemical performances

Teng Wang, Bingjun Jin, Zhengbo Jiao, Gongxuan Lu, Jinhua Ye, and Yingpu Bi[*]
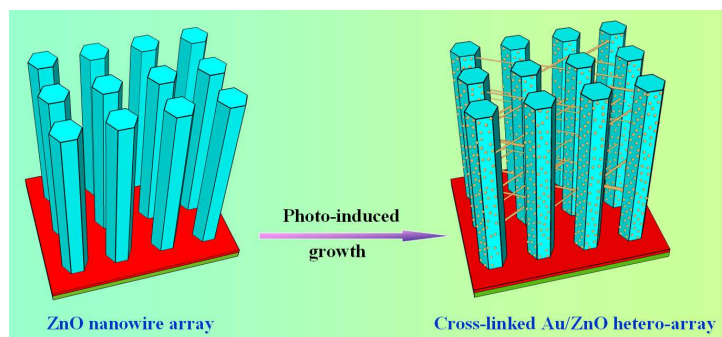
Herein, we demonstrate that ZnO nanowire arrays could be rationally connected with each other by thin Au nanowires to construct a novel cross-linked hetero-structure by a simple photo-directed growth strategy, which exhibit much higher visible light photocurrent density than both pure ZnO nanowire arrays and traditional Au nanoparticles/ZnO nanowire heterostructures.